An electrochemical sensor based on poly (L-Cysteine)@AuNPs @ reduced graphene oxide nanocomposite for determination of levofloxacin

6 authors, including:

Mohammad Hossein Ghanbari
Kharazmi University
11 PUBLICATIONS   **29** CITATIONS

SEE PROFILE

Hossein Sobati
Baqiyatallah University of Medical Sciences
18 PUBLICATIONS   **57** CITATIONS

SEE PROFILE

Mehdi Rahimi-Nasrabadi
Imam Hossein University
181 PUBLICATIONS   **3,557** CITATIONS

SEE PROFILE

Farhad Ahmadi
Iran University of Medical Sciences
133 PUBLICATIONS   **2,431** CITATIONS

SEE PROFILE

Some of the authors of this publication are also working on these related projects:

Asghar Hosseininia View project

Analysis of digger scorpions View project

Accepted Manuscript

An electrochemical sensor based on poly (l-Cysteine)@AuNPs @ reduced graphene oxide nanocomposite for determination of levofloxacin

Mohammad Hossein Ghanbari, Alireza Khoshroo, Hossein Sobati, Mohammad Reza Ganjali, Mehdi Rahimi-Nasrabadi, Farhad Ahmadi

Please cite this article as: M.H. Ghanbari, A. Khoshroo, H. Sobati, et al., An electrochemical sensor based on poly (l-Cysteine)@AuNPs @ reduced graphene oxide nanocomposite for determination of levofloxacin, Microchemical Journal, https://doi.org/10.1016/j.microc.2019.03.016

An electrochemical sensor based on poly (L-Cysteine)@AuNPs @ reduced graphene oxide nanocomposite for determination of levofloxacin

Mohammad Hossein Ghanbari[1,2], Alireza Khoshroo[3], Hossein Sobati[4], Mohammad Reza Ganjali[5,6], Mehdi Rahimi-Nasrabadi[1,2,*], Farhad Ahmadi[7,8,*]

[1]*Chemical Injuries Research Center, Systems Biology and Poisonings Institute, Baqiyatallah University of Medical Sciences, Tehran, Iran*
[2]*Faculty of Pharmacy, Baqiyatallah University of Medical Sciences, Tehran, Iran*
[3]*Pharmaceutical Sciences Research Center, School of Pharmacy, Kermanshah University of Medical Sciences, Kermanshah, 6734667149, Iran*
[4]*Health Research Center, Lifestyle Institute, Baqiyatallah University of Medical Sciences, Tehran, Iran*
[5]*Center of Excellence in Electrochemistry, University of Tehran, Tehran, Iran*
[6]*Biosensor Research Centre, Endocrinology & Metabolism Molecular and Cellular Research Institute, Tehran University of Medical Sciences, Tehran, Iran*
[7]*Physiology Research Center, Iran University of Medical Sciences, Tehran, Iran*
[8]*Department of Medicinal Chemistry, School of Pharmacy-International Campus, Iran University of Medical Sciences, Tehran, Iran*

[*] Corresponding author

E–mails: rahiminasrabadi@gmail.com, rahimi@bmsu.ac.ir (M. Rahimi-Nasrabadi), farhadahmadi55@gmail.com (F. Ahmadi); Tel.: +98 9122582077, +98 2182483409

Abstract

A novel electrochemical sensor has been developed for levofloxacin (LEV), by coating a glassy carbon electrode (GCE) with a film of poly (L-Cysteine)@Au NPs@reduced graphene oxide. Cyclic voltammetry, electrochemical impedance spectroscopy, UV-Vis spectroscopy, FT-IR spectroscopy and electron scanning microscope imaging were used for general surface characterization over the successive electrode modification steps. The electrochemical properties of the LEV was monitored by performing cyclic voltammetry (CV) experiments. The CVs showed one oxidation peak at 1.0 V during the anodic potential scan, which was attributed to LEV. Differential pulse voltammetry experiments using the modified electrode produced linear response in two concentration windows of 1.0×10^{-11} M and 1.0×10^{-4} (LEV), with detection limits of 3.0×10^{-12} M for LEV. The GCE modified through coating with a film of poly(l-cys)/AuNPs/rGO/GCE was found to offer high stability, reproducibility, and repeatability, as well as selectivity for LEV in mixed samples, and was successfully used in the analysis of the LEV in synthetic blood serum , with recovery values of around 99%.

Keywords: Sensor, Reduced graphene oxide, Poly (L-Cysteine), AuNPs, Levofloxacin.

1. Introduction

A somewhat new recent concern is the emergence of the incremental occurrence of antibiotic-resistant bacterial infections, as a result of over-prescription and neglected overuse of antibiotics for humans and animals. The latter, i.e. the widespread application of antibiotics in agriculture and aquaculture has created worries about the residual contents of these materials in animal-based foods. This can lead to direct toxic effects or create pathogen resistance and probable allergic hypersensitivity in humans [1,2]. There, hence, has been the need for sensitive and selective methods for the analysis of antibiotics, as means for monitoring the proper use of antibiotics, public health, as well as for developing and selecting new drugs [3,4]. (−)-(S)-9-fluoro-2.3-dihydro-3-methyl-10-(4-ethyl-1-piperazinyl)-7-oxo-7H pyrido[2,3,4-de]-1,4-benzoxazine-6-carboxilic acid hemihydrate, also widely known as levofloxacin (LEV) is a common orally administered third-generation fluoroquinolones antibiotic. Being the S-(-) the optical isomer of ofloxacin, LEV is prescribed in the case of respiratory, urinary, skin and soft tissue infections [5], further to being associated with various clinical and microbiological applications [6].

Various reports have been published on the determination of LEV based on HPLC [7], LC-MS [8], spectrophotometry methods [8], etc. Electrochemical techniques, which offer advantages of high speed, ease of use and low cost [9-12], have also been used for determination of different compounds through the application of glassy carbon electrodes (GCEs) [13], immunosensors [14], as well as electrodes modified with a conductive polymer [15], MWCNT modified electrode [16], and graphene based modified electrode [17,18]. The extraordinary properties of nanostructures have expanded their use in various fields like catalyst, photocatalyst, supercapacitor and other energy storage systems and many other fields [19-24]. One of this interesting field is expanding chemical and electrochemical sensors based on different nanostructures. Unique properties of graphene such as surface

3

area, outstanding electrical conductivity, exceptional mechanical property, and easy surface modification allow it to be used in potential electrochemical applications [9,25,26]. From the most recent progress in reduced graphene oxide nanocomposites and their sensor application can refer to poly N-methylthionine /electrochemically reduced graphene oxide (ERGO) composite by the combination of electrochemical reduction and catalytic polymerization: ERGO acts as both the efficient template and catalyst for the N-methylthionine polymerization [27]. Furthermore, the PNMTh/rGO nanocomposite used as a novel electrochemical sensing material for highly sensitive sensor [9]. Recently, the use of organic functionalized groups and biological molecules as the immobilization matrix in the electrode fabrication procedure has attracted considerable attention, owing to their multiple active sites, selectivity, sensitivity, and the chemical stability. LCysteine (L-Cys) is the semi-essential protein genic amino acids which as an electrochemical sensor material, provides tunable conductivity and rapid electron transfer as well as creates abundant active sites for binding analytes [28, 29]. A limited number of reports exist on the electrochemical analysis of LEV using devices based on metallic or composite metallic oxide materials. A prevalent class of instruments prepared based on this concept are electrochemical sensors modified with nanoparticles. This is due to advantages of these materials including high surface and stability, as well as unique electrochemical properties [30]. Reports are indicating the applicability of gold nanoparticles as oxidation catalysts, as well as, for enhancing the sensitivity and stability of electrochemical sensors [31–33].

In this study, we evaluated the application of gold nanoparticles as a catalytically active material for modifying LEV electrodes. The electrodes were primarily modified using poly (L-Cysteine) @reduced graphene oxide to form a stable matrix for Au nanoparticles. The synergy of the good electro-catalytic ability the nanoparticles, and the high surface area of the (L-Cysteine) @ reduced graphene oxide was found to significantly improve the

4

detection limit of the electrode, which was successfully used in the analysis of LEV in the blood serum samples.

2. Experimental section

2.1. Chemicals and instruments

Analytical grade chemicals were procured from various companies and used without any treatment. The 0.1 M phosphate buffer solution (PBS) used as the electrolyte was prepared using KH_2PO_4 and K_2HPO_4 obtained from Merck. The LEV sample was from Merck Co. L-Cysteine (Merck), Graphite powders (USA), LEV (Merck). $HAuCl_4.3H_2O$ from Merck Co. Deionized water was used throughout the research. Fresh frozen human blood serum samples were obtained from Iranian Blood Transfusion Organization (Tehran-Iran) and stored frozen until the assay time. The samples were diluted with 0.1 mol L^{-1} PBS (with a ratio of 1:20). A stock 1.0×10^{-3} M LEV solution in water was prepared and used for preparing other solutions. The electrochemical measurements were carried out with a Palm Sens (Em state 3+) potentiostat. The electrochemical system was a three-electrode setup composed of a modified (or unmodified) glassy carbon electrode (as the working electrode), a Pt wire as the counter electrode, and an Ag/AgCl/3.0 M KCl reference electrode. pH measurements were performed under ambient conditions using a Metrohm, pH Lab 827 digital pH/mV/Ion meter.

2.2. Fabrication of poly (l-cys)/AuNPs/rGO/GCE

Initially bare GCEs were polished using alumina particles to obtain a shiny surface. Next the electrodes were sonicated in a deionized water bath for 2 minutes, and eventually successively cleaned in 1:1 nitric acid, alcohol and deionized water baths, by sonication. GO was obtained through the Hummer method, which involves oxidizing graphite powder using a combination of $KMnO_4$, $NaNO_2$, and concentrated H_2SO_4 [34]. The product was repeatedly washed under centrifugation at 5000 rpm (for 20 min), and then dispersed in deionized water

5

and sonicated to obtain a thin layer GO. The separated GO was then dried at 40 ℃ overnight. The product was evaluated using SEM, FT-IR, and UV-Vis techniques.

5 µl of a 1 mg mL^{-1} GO dispersion was dropped onto and distributed on the surface of the GCE, and then allowed to dry at room temperature. The GO was reduced (to rGO) through applying 100 cyclic voltammetric scans in the range of 0.0 to −1.5 V, in a 0.1 M PBS (pH=5.0) and then the electrodes were rinsed with deionized water and left to dry at ambient conditions, before the rGO layer was electrodeposited with Au nanoparticles. To this end 20 potential scans at 50 mV s^{-1} were performed from −0.2 to −1.3 V. These experiments were performed in a 0.1 M PBS (pH=7.0) also containing 0.1 mM of HAuCl$_4$ [35]. The resulting assembly (i.e. GCE/rGO/AuNPs) was eventually washed, before being coated with an electro-polymerized film of L-cys through 10 CV runs in 0.1 M PBS (pH=6.0) further containing 1.0 mM l-cys, in the potential range −1.5 to +2.2 V at 100 mV/s. The resulting poly (l-cys)/AuNPs/rGO/GCE was then dried in air and kept under ambient conditions. The fabrication process of the electrochemical sensor is illustrated in scheme.1

Insert Scheme.1

3. Results and discussion

3.1. Characterizing of GO and rGO samples

The UV−Vis spectra acquired for GO samples are illustrated in Figure 1A. The absorptions corresponding to the π−π* and n−π* transitions of GO can be seen around 227 and 300 nm [36,37]. Figure 1B shows the FT-IR spectra of GO. As can be seen the characteristic peaks of GO at 3382, 1708, 1226, and 1076 cm^{-1} correspond to the stretching vibrations of O−H, carboxylic acid C=O, C−OH, and C−O and the signal at about 1363 cm^{-1} corresponds to the deformation of the O-H bond. The band at 3380−3600 cm^{-1} which related to the stretching vibration of hydrogen bond due to the presence of hydroxyl groups [38-40].

6

Insert Fig.1

3.2. Characterization of poly (l-cys)/AuNPs/rGO/GCE

Applying the conditions of cyclic voltammetry can be used as an efficient approach for synthesis of different conducting polymers on the surface of working electrodes. The CV curves obtained during the electro-polymerization of l-cys using the AuNPs/rGO/GCE working electrode can be seen in Figure 2. It is easy to see that the current increases with increasing CV cycles. This is a typical observation in the case of the electrochemical preparation of conductive polymers, and is considered as proof of the successful formation of the polymer film on the surface of AuNPs/ rGO/GCE.

Insert Fig.2

Once the electrode was formed, its electrochemical behavior was evaluated through CV runs in a $[Fe(CN)_6]^{3-/4-}$ solution as a redox probe. The results obtained in a 0.1 mM solution of $[Fe(CN)_6]^{3-/4-}$ (1:1) also containing 0.1 M of potassium chloride at scan rate of 50 mV/s can be seen in Figure 3A. After modified of GCE, the peak current increased obviously (curve d) due to the electrocatalytic effect of Poly (l-cys)/AuNPs/rGO/GCE for oxidation of $[Fe(CN)_6]^{3-/4-}$, this can be ascribed to the fact that Poly (l-cys)/AuNPs/rGO can significantly enhance the effective surface area and facilitate the electron transfer.

Insert Fig.3

For further characterizing the electrode, it was used in electrochemical impedance spectroscopy (EIS) tests at a potential of 0.23 V and in the range of 0.1 Hz to 10000 Hz. Figure 3B illustrates the Nyquist plots obtained using bare GCE (a), rGO/GCE(b), AuNPs/rGO/GCE(c) and Poly (l-cys)/AuNPs/rGO/GCE(d) in a 5 mM $[Fe(CN)_6]^{3-/4-}$ solution

also containing 0.1 M of KCl. It can be seen that on the Poly (l-cys)/AuNPs/rGO/GCE (curve d, R_{ct} = 240 Ω) the value of R_{ct} is smaller than to AuNPs/rGO/GCE (curve c, R_{ct} = 392 Ω) and bare GCE (curve a, R_{ct} = 920 Ω). This is due to the excellent catalytical property of Poly (l-cys)/AuNPs/rGO that formed a high electron conduction pathway between the electrode and $[Fe(CN)_6]^{3-/4-}$.

The morphology of the different electrodes were studied through SEM and the results are presented in Figure 4. According to Figure 4a the GCE has an amorphous carbon morphology, while Figure 4b reflects a typical crumpled/wrinkled morphology for graphene with enhanced electrode surface area. Then, Au nanoparticles were successfully deposited on the GCE surface by the CV technique (Figure 4c), after electro polymerizing l-cys onto the rGO/GCE Figure 4d, a conductive polymeric film was formed on the wrinkled rGO containing the final Poly (l-cys)/AuNPs/rGO/GCE.

Insert Fig.4

3.3. Properties of the Poly (l-cys)/AuNPs/rGO/GCE

The differential pulse voltamograms (DPV) recorded in blank PBS (pH=6.5) and also 0.01 mM solutions of LEV in PBS (pH=6.5) using bare GCE and Poly (l-cys)/AuNPs/rGO/GCE as the working electrodes. The results of the DPV tests at 100 mV/s are presented in Figure 5A. Clearly no redox peaks are present in the case of the blank sample with both bare and modified electrodes (curves a and b). Yet the magnitude of the background current was higher with the modified GCE, which was attributed to the faradic current, reflecting significant changes in the surface properties of the electrode as a result of modification. Figure 5A (c and d) clearly shows that the anodic peak current in LEV-containing sample was significantly enhanced with the modified poly (l-cys)/AuNPs/rGO/GCE. Figure 5B shown the DPV recorded in 0.01mM solutions of LEV in

8

PBS (pH=6.5) using unmodified GCE, as well as GCE/rGO, GCE/rGO/Au NPs and poly (l-cys)/AuNPs/rGO/GCE.

Insert Fig.5

3.4. Influence of the potential scan rate

In order to evaluate the dependence between the electrochemical behavior of poly (l-cys)/rGO/GCE and the potential scan rate, different CV were performed by applying potential scan rates in the range of 40 to 500 mVs^{-1} using 1.0×10^{-5} M LEV solution in 0.1 M PBS (Figure 6). According to plots of the peak current against the square root of the potential scan rate (Δipa vs. v$^{\frac{1}{2}}$), based on experimental data LEV oxidation is a diffusion controlled processes [41]. Moreover, the peak current potential of LEV had a shift to more positive values with increasing the scan rate, reflecting the irreversibility of the process [42].

Insert Fig.6

3.5. Effect of pH

The effects of the pH of the electrolyte (i.e. 0.1 M PBS) on the peak current and potential of the LEV was studied in the range of 5.5 to 8.0 and the observations are presented in Figure 7. It can be seen that increasing the pH in this range enhances the peak current up to a pH of 6.5 (Figure 7A). A plot of E vs pH (Figure 7B), shows that the peak potential moves in the negative direction with increasing the pH, reflecting the occurrence of a prior chemical (proton transfer) reaction (Scheme 2). The optimal peak current was observed at pH=6.5, which was used as the optimal value in further studies.

Insert Fig.7

3.6. Performance of the electrode

3.6.1. Stability and repeatability

The modified electrode was found to produce stable responses even after 20 days, when kept in a sealed vessel. During the test period DPV tests were conducted using the electrode every four days using a 1.0 μM LEV solution in PBS (pH=6.5). Based on the results the modified electrode was still capable of maintaining 88.0% of its original current response, after the period under the test condition. To evaluate the repeatability of the response of the modified electrode the peak currents of 8 replicate DPV experiments of a 1.0 μM LEV solution in PBS (pH=6.5) were measured and compared. The relative standard deviation (RSD) of the results was determined to be 1.8%, reflecting the good repeatability of the modified electrode. The reports Comparison of repeatability and stability for determination of LEV at various modified electrodes can be seen (Table 1).

3.6.2. Voltammetric determination of levofloxacin on poly (l-cys)/AuNPs/rGO/GCE

Figure 8A shows the DPV curves of LEV at various concentrations from 1.0×10^{-7} to 1.0×10^{-4} M and Figure 8B shows the DPV curves of LEV at various concentrations from 1.0×10^{-11} to 1.0×10^{-7} M. The plot of I_{pa} against concentration of LEV shows a two linear dynamic range 1.0×10^{-7} to 1.0×10^{-4} M with a R^2 value of 0.996. The linear regression equation for this range is I (μA) = 9.148 C+10.6) and 1.0×10^{-11} to 1.0×10^{-7} M with a R^2 value of 0.994. The linear regression equation for this range is I (μA) = 0.2489C+2.252). The detection limit of the method was calculated to be 3.0×10^{-12} M with the signal to noise ratio of 3), The literature reports different studies involving the individual determination of LEV with modified electrodes can be seen (Table 2), the proposed sensor exhibited excellent analytical performance for the determination of LEV, with limits of detection and or linear concentration ranges similar to, or better than, those reported previously.

Insert Fig.8

10

3.7. Interference studies

The influences of various foreign species (inorganic ions and organic compounds commonly existed in pharmaceuticals and biological samples) on the determination of LEV were investigated. The tolerance limit was defined as the concentration ratio of interference /LEV causing less than ±3.0% relative error. The results indicated as follows: the tolerance limit of additives to 1 μM LEV was ∼300 for Na^+, ∼300 for K^+ ∼150 for glucose, ∼100 for fructose, ∼60 for valine, ∼120 for urea, ∼130 for SO_4^{2-}, ∼130 for NO_3^-, ∼20 for ascorbic acid and ∼20 for uric acid (Figure 9). But equal molar of norfloxacin, ciprofloxacin, enoxacin, and lomefloxacin cause serious interference.

Insert Fig.9

3.8. Analysis of real samples

The LEV content of blood samples were determined using the electrochemical sensor, after highly diluting the blood serums with PBS (pH=6.5) using the standard addition method. The recovery values were determined by comparing the measured concentrations with their known values. The RSD and recovery values reported in Table 3 were calculated from the results obtained for five replicate tests in three concentrations levels. The recovery values fell in the range of 96% to 102.2%. This indicates the good accuracy of the electrode which makes it a highly potential candidate for real sample analyses.

4. Conclusions

The developed modified GCE for the analysis LEV (i.e. poly (l-cys)/AuNPs/rGO/GCE could be the first of its kind for the electrochemical analysis of LEV. The sensing platform presented an appreciable ability to show many advantages such as high surface area, efficient catalytic ability and subsequently, wide linear range, low LOD, high

stability and reproducibility in the LEV detection. The poly (l-cys)/AuNPs/rGO/GCE was effectively used for the determination of LEV content of human blood serum through standard addition method. Overlay, it can be easily extended and it has the potential to be applied for detecting other targets with acceptable results.

References

[1]   H. Yan, F. Qiao, K.H. Row, Molecularly imprinted-matrix solid-phase dispersion for selective extraction of five fluoroquinolones in eggs and tissue, Anal. Chem. 79 (2007) 8242–8248.

[2]   F.M. Wagenlehner, O. Umeh, J. Steenbergen, G. Yuan, R.O. Darouiche, Ceftolozane-tazobactam compared with levofloxacin in the treatment of complicated urinary-tract infections, including pyelonephritis: a randomised, double-blind, phase 3 trial (ASPECT-cUTI), Lancet. 385 (2015) 1949–1956.

[3]   M.D. Hernando, M. Mezcua, A.R. Fernández-Alba, D. Barceló, Environmental risk assessment of pharmaceutical residues in wastewater effluents, surface waters and sediments, Talanta. 69 (2006) 334–342.

[4]   Y. Yuan, X. Zhao, S. Liu, Y. Li, Y. Shi, J. Yan, et al., A fluorescence switch sensor used for D-Penicillamine sensing and logic gate based on the fluorescence recovery of carbon dots, Sensors Actuators B Chem. 236 (2016) 565–573.

[5]   A.F. Faria, M.V.N. de Souza, M. V de Almeida, M.A.L. de Oliveira, Simultaneous separation of five fluoroquinolone antibiotics by capillary zone electrophoresis, Anal. Chim. Acta. 579 (2006) 185–192.

[6]   J.P. Gisbert, F. De La Morena, Systematic review and meta- analysis: levofloxacin- based rescue regimens after Helicobacter pylori treatment failure, Aliment. Pharmacol. Ther. 23 (2006) 35–44.

[7]   U. Neckel, C. Joukhadar, M. Frossard, W. Jäger, M. Müller, B.X. Mayer, Simultaneous determination of levofloxacin and ciprofloxacin in microdialysates and plasma by high-performance liquid chromatography, Anal. Chim. Acta. 463 (2002) 199–206.

[8]   J.A.O. González, M.C. Mochón, F.J.B. de la Rosa, Spectrofluorimetric determination of levofloxacin in tablets, human urine and serum, Talanta. 52 (2000) 1149–1156.

[9]   Liu, Yinqiu, et al. "Synthesis of a poly (N-methylthionine)/reduced graphene oxide nanocomposite for the detection of hydroquinone." Materials Chemistry and Physics 223 (2019): 548-556.

[10]   A. Khoshroo, M. Mazloum-Ardakani, M. Forat-Yazdi, Enhanced performance of label-free electrochemical immunosensor for carbohydrate antigen 15-3 based on

catalytic activity of cobalt sulfide/graphene nanocomposite, Sensors Actuators B Chem. 255 (2018) 580–587.

[11] M.R. Ganjali, M.B. Gholivand, M. Rahimi-Nasrabadi, B. Maddah, M. Salavati-Niasari, F. Ahmadi, Synthesis of a new octadentates Schiff's base and its application in construction of a highly selective and sensitive lanthanum (III) membrane sensor, Sensor Letters 4 (2006) 356-363.

[12] A. Khoshroo, L. Hosseinzadeh, A. Sobhani‑Nasab, M. Rahimi-Nasrabadi, H. Ehrlich, Development of electrochemical sensor for sensitive determination of oxazepam based on silver-platinum core–shell nanoparticles supported on graphene, Journal of Electroanalytical Chemistry 823 (2018) 61-66.

[13] M. Rahimi-Nasrabadi, A. Khoshroo, M. Mazloum-Ardakani, Electrochemical determination of diazepam in real samples based on fullerene-functionalized carbon nanotubes/ionic liquid nanocomposite, Sensors Actuators B Chem. 240 (2017) 125–131.

[14] J. Amani, A. Khoshroo, M. Rahimi-Nasrabadi, Electrochemical immunosensor for the breast cancer marker CA 15–3 based on the catalytic activity of a CuS/reduced graphene oxide nanocomposite towards the electrooxidation of catechol, Microchim. Acta. 185 (2018) 79.

[15] J. Amani, M. Maleki, A. Khoshroo, A. Sobhani-Nasab, M. Rahimi-Nasrabadi, An electrochemical immunosensor based on poly p-phenylenediamine and graphene nanocomposite for detection of neuron-specific enolase via electrochemically amplified detection, Anal. Biochem. 548 (2018) 53–59.

[16] M. Mazloum-Ardakani, S.H. Ahmadi, Z.S. Mahmoudabadi, A. Khoshroo, Nano composite system based on fullerene-functionalized carbon nanotubes for simultaneous determination of levodopa and acetaminophen, Measurement. 91 (2016) 162–167.

[17] J. Li, J. Jiang, Z. Xu, M. Liu, S. Tang, C. Yang, et al., Facile synthesis of Ag@Cu$_2$O heterogeneous nanocrystals decorated N-doped reduced graphene oxide with enhanced electrocatalytic activity for ultrasensitive detection of H$_2$O$_2$, Sensors Actuators B Chem. 260 (2018) 529–540.

[18] J. Li, Z. Xu, M. Liu, P. Deng, S. Tang, J. Jiang, et al., Ag/N-doped reduced graphene oxide incorporated with molecularly imprinted polymer: An advanced electrochemical sensing platform for salbutamol determination, Biosens. Bioelectron. 90 (2017) 210–216.

[19] M. Eghbali-Arani, A. Sobhani-Nasab, M. Rahimi-Nasrabadi, S. Pourmasoud, Green Synthesis and Characterization of SmVO$_4$ Nanoparticles in the Presence of Carbohydrates As Capping Agents with Investigation of Visible-Light Photocatalytic Properties, J. Electron. Mater. 47(2018) 3757-3769.

[20] M. Rahimi-Nasrabadi, M. Behpour, A. Sobhani-Nasab, M. Rangraz Jeddy, Nanocrystalline Ce-doped copper ferrite: synthesis, characterization, and its photocatalyst application, J. Mater. Sci. Mater. Electron. 27 (2016) 11691–11697.

[21] M. Rahimi-Nasrabadi, M. Behpour, A. Sobhani-Nasab, S.M. Hosseinpour-Mashkani, $ZnFe_{2-x}La_xO_4$ nanostructure: synthesis, characterization, and its magnetic properties, J. Mater. Sci. Mater. Electron. 26 (2015) 9776-9781.

[22] M. Aghazadeh, I. Karimzadeh One-pot electro-synthesis and characterization of chitosan capped superparamagnetic iron oxide nanoparticles (SPIONs) from ethanol media, Curr. Nanosci. 14 (2018), 42-49

[23] A. Sobhani-Nasab, S. Pourmasoud, F. Ahmadi, M. Wysokowski, T. Jesionowski, H. Ehrlich, M. Rahimi-Nasrabadi[*], Synthesis and characterization of $MnWO4/TmVO_4$ ternary nano-hybrids by an ultrasonic method for enhanced photocatalytic activity in the degradation of organic dyes, Mater. Lett. 238 (2019) 159–162.

[24] M. Aghazadeh, One-step cathodic electrosynthesis of surface capped Fe3O4 ultra-fine nanoparticles from ethanol medium without using coating agent, Mater. Lett. 211 (2018) 225-229.

[25] M. Rostami, M. Rahimi-Nasrabadi, M.R. Ganjali, F. Ahmadi, A. Fallah Shojaei, M. Delavar Rafiee, Facile synthesis and characterization of TiO_2–graphene–$ZnFe_{2-x}Tb_xO_4$ ternary nano-hybrids, J. Mater. Sci. 52 (2017) 7008–7016.

[26] H.R Naderi, A. Sobhani-Nasab, M. Rahimi-Nasrabadi, M.R. Ganjali, Decoration of Nitrogen-doped Reduced Graphene Oxide with Cobalt Tungstate Nanoparticles for Use in High-Performance Supercapacitors, Appl. Surf. Sci. 423 (2017) 1025–1034.

[27] C. Chen, Z. GanKang, K. Zhou, Z. Ma, Y. Liu, Y. Gao, Catalytic polymerization of N-methylthionine at electrochemically reduced graphene oxide electrodes, Electrochim. Acta 283 (2018) 1649-1659.

[28] M. Arvand, M. Sanayeei, S. Hemmati, Label-free electrochemical DNA biosensor for guanine and adenine by ds-DNA/poly (L-cysteine)/Fe_3O_4 nanoparticles-graphene oxide nanocomposite modified electrode, Biosen. Bioelectron. 102 (2018) 70-79.

[29] B. Hatamluyi, F. Lorestani, Z. Es'haghi. Au/Pd@ rGO nanocomposite decorated with poly (L-Cysteine) as a probe for simultaneous sensitive electrochemical determination of anticancer drugs, Ifosfamide and Etoposide, Biosen, Bioelectron, 120 (2018) 22-29.

[30] X. Luo, A. Morrin, A.J. Killard, M.R. Smyth, Application of nanoparticles in electrochemical sensors and biosensors, Electroanalysis 18 (2006) 319–326.

[31] A. Yu, Z. Liang, J. Cho, F. Caruso, Nanostructured electrochemical sensor based on dense gold nanoparticle films, Nano Lett. 3 (2003) 1203–1207.

[32] M. Mazloum-Ardakani, B. Barazesh, A.R. Khoshroo, M. Moshtaghiun, M.H. Sheikhha, A new composite consisting of electrosynthesized conducting polymers, graphene sheets and biosynthesized gold nanoparticles for biosensing acute lymphoblastic leukemia, Bioelectrochem. 121 (2018) 38–45.

[33]   J. Zou, G.-Q. Zhao, J. Teng, Q. Liu, X.-Y. Jiang, F.-P. Jiao, et al., Highly sensitive detection of bisphenol A in real water samples based on in-situ assembled graphene nanoplatelets and gold nanoparticles composite, Microchem. J. (2018).

[34]   J. Guerrero-Contreras, F. Caballero-Briones, Graphene oxide powders with different oxidation degree, prepared by synthesis variations of the Hummers method, Mater. Chem. Phys. 153 (2015) 209–220.

[35]   Y. Zhang, G.M. Zeng, L. Tang, J. Chen, Y. Zhu, X.X. He, et al., Electrochemical sensor based on electrodeposited graphene-Au modified electrode and nanoAu carrier amplified signal strategy for attomolar mercury detection, Anal. Chem. 87 (2015) 989–996.

[36]   Y. Xu, C.-Y. Chen, Z. Zhao, Z. Lin, C. Lee, X. Xu, et al., Solution processable holey graphene oxide and its derived macrostructures for high-performance supercapacitors, Nano Lett. 15 (2015) 4605–4610.

[37]   V. Loryuenyong, C. Saewong, C. Aranchaiya, A. Buasri, The improvement in mechanical and barrier properties of poly (vinyl alcohol)/graphene oxide packaging films, Packag. Technol. Sci. 28 (2015) 939–947.

[38] H.R Naderi, A. Sobhani-Nasab, M. Rahimi-Nasrabadi, M.R. Ganjali, Decoration of Nitrogen-doped Reduced Graphene Oxide with Cobalt Tungstate Nanoparticles for Use in High-Performance Supercapacitors, Applied Surface Science 423 (2017) 1025–1034.

[39] M. Rahimi-Nasrabadi, M. Rostami, F. Ahmadi, A.F. Shojaie, M.D. Rafiee, Synthesis and characterization of $ZnFe_2-xYbxO_4$–graphene nanocomposites by sol–gel method, Journal of Materials Science: Materials in Electronics 27 (2016) 11940-11945.

[40]   M. Rahimi-Nasrabadi, H.R. Naderi, M. Sadeghpour Karimi, F. Ahmadi, S. M. Pourmortazavi, Cobalt carbonate and cobalt oxide nanoparticles synthesis, characterization and supercapacitive evaluation, J. Mater. Sci. Mater. Electron. 28 (2017) 1877–1888.

[41]   E. Laviron, General expression of the linear potential sweep voltammogram in the case of diffusionless electrochemical systems, J. Electroanal. Chem. Interfacial Electrochem. 101 (1979) 19–28. doi:http://dx.doi.org/10.1016/S0022-0728(79)80075-3.

[42]   A.J. Bard, L.R. Faulkner, Electrochemical Methods: Fundamentals and Applications, 2nd ed., Wiley, 2000.

[43]   W. Wen, D.-M. Zhao, X.-H. Zhang, H.-Y. Xiong, S.-F. Wang, W. Chen, et al., One-step fabrication of poly (o-aminophenol)/multi-walled carbon nanotubes composite film modified electrode and its application for levofloxacin determination in pharmaceuticals, Sensors Actuators B Chem. 174 (2012) 202–209.

[44]   L. Tang, Y. Tong, R. Zheng, W. Liu, Y. Gu, C. Li, R. Chen, Z. Zhang, Ag nanoparticles and electrospun CeO2-Au composite nanofibers modified glassy carbon

electrode for determination of levofloxacin, Sensor. Actuat. B: Chem. 203 (2014) 95-101.

[45] L. Han, Y. Zhao, C. Chang, F. Li, A novel electrochemical sensor based on poly (p-aminobenzene   sulfonic acid)-reduced graphene oxide composite film for the sensitive and selective detection of levofloxacin in human urine, J. Electroanal. Chem. 817 (2018) 141-148.

[46] A. Radi, M.A. El Ries, S. Kandil, Electrochemical study of the interaction of levofloxacin with DNA, Anal. Chim. Acta 495.1-2 (2003) 61-67.

[47] J. Borowiec, K. Yan, C.-C. Tin, J. Zhang, Synthesis of PDDA functionalized reduced graphene oxide decorated with gold nanoparticles and its electrochemical response toward levofloxacin, J. Electrochem. Soc. 162 (2015) H164–H169.

[48] F.C. Moraes, T.A. Silva, I. Cesarino, M.R. V Lanza, S.A.S. Machado, Antibiotic detection in urine using electrochemical sensors based on vertically aligned carbon nanotubes, Electroanalysis. 25 (2013) 2092–2099.

[49] V. Cesarino, I. Cesarino, F.C. Moraes, S.A.S. Machado, L.H. Mascaro, Carbon nanotubes modified with SnO2 rods for levofloxacin detection, J. Braz. Chem. Soc. 25 (2014) 502–508.

[50] F. Wang, L. Zhu, J. Zhang, Electrochemical sensor for levofloxacin based on molecularly imprinted polypyrrole–graphene–gold nanoparticles modified electrode, Sensors Actuators B Chem. 192 (2014) 642–647.

Legends for the Figures:

Fig. 1: (A) the UV−Vis spectra of GO and (B) the FT-IR spectra of GO.

Fig. 2: A) CVs for electrochemical reduced GO to rGO through applying 100 cyclic voltammetric scans in the range of 0.0 to −1.5 V, in a 0.1 M PBS (pH=5.0) at scan rate 100 mV s^{-1}, B) CVs for electrodeposited Au nanoparticles onto the rGO/GCE in 0.1 M PBS (pH=7.0) also containing 0.1 mM of HAuCl$_4$ after 20 cycles in the range of −0.2 to −1.3 V at scan rate 50 mV s^{-1}. C) CVs for electrochemical polymerization of l-cys in 0.1 M PBS (pH 6.0) containing 1.0 mM l-cys onto AuNPs/rGO/GCE After 10 cycles in the range of −1.5 to +2.2 V at scan rate 100 mV s^{-1}.

Fig. 3: (A) the CVs and (B) electrochemical impedance spectra of bare GCE (a), rGO/GCE(b), AuNPs/rGO/GCE(c) and Poly (l-cys)/AuNPs/rGO/GCE(d) in 5.0 mM [Fe(CN)$_6$]$^{3-/4-}$ solution containing 0.10 M KCl.

Fig. 4: SEM images of the working surface area for: bare GCE (a), rGO/GCE(b), AuNPs/rGO/GCE(c) and Poly (l-cys)/AuNPs/rGO/GCE(d).

Fig. 5: A) DPV of the bare GCE in blank PBS (pH=6.5) (a) and in presence of 0.01 mM LEV (c) and GCE/rGO/Au NPs/Poly (l-cys) in blank PBS (pH=6.5) (b) and in presence of 0.01 mM LEV (d). B) DPV recorded in PBS (pH=6.5) and also 0.01 mM solution of LEV in PBS (pH=6.5) using bare GCE (a), GCE/rGO (b), GCE/rGO/Au NPs (c), and poly (l-cys)/AuNPs/rGO/GCE (d).

Fig. 6: CVs of poly (l-cys)/AuNPs/rGO/GCE in PBS (pH 6.5) containing 1.0×10^{-5} LEV at various scan rates; from inner to outer scan rates of 40-500 mVs^{-1}, respectively.

Fig. 7: Cyclic voltammograms of 0.1 mM LEV recorded from pH 5.5 to 8 at a scan rate of 100 mV/s.

Fig. 8: (A) Differential pulse voltammograms of GCE/rGO/AuNPs/Poly(l-cys) in various LEV concentrations in the range 1.0×10^{-7} to 1.0×10^{-4} M (B) Differential pulse voltammograms of GCE/rGO/AuNPs/Poly(l-cys) in various LEV concentrations in the range

1.0×10^{-11} to 1.0×10^{-7} M. (The DPV parameters: E_{step} = 0.005 V, E_{pulse} = 0.06 V, t_{pulse} = 0.02 s, Scan rate = 0.1 V/s).

**Fig. 9:** Histogram of the change of (A) concentration vs. different probable interferences (150 μmol L^{-1} of glucose, 100 μmol L^{-1} of fructose, 120 μmol L^{-1} of urea, 130 μmol L^{-1} of SO_4^{2-} and NO_3^-, 300 μmol L^{-1} of Na^+ and K^+, 60 μmol L^{-1} of valine, 20 μmol L^{-1} of ascorbic acid and uric acid) towards LEV (1 μmol L^{-1}) and (B) Influences of some possible interferences on the response of 1.0 μM LEV. i and i_0 represent peak current responses of LEV in presence and absence of interferences, respectively.

Scheme 1: Schematic exhibition of fabrication process of the poly l-cys/Au NPs/rGO/GCE.
Scheme 2. Proposed reaction mechanism for oxidation of LEV.
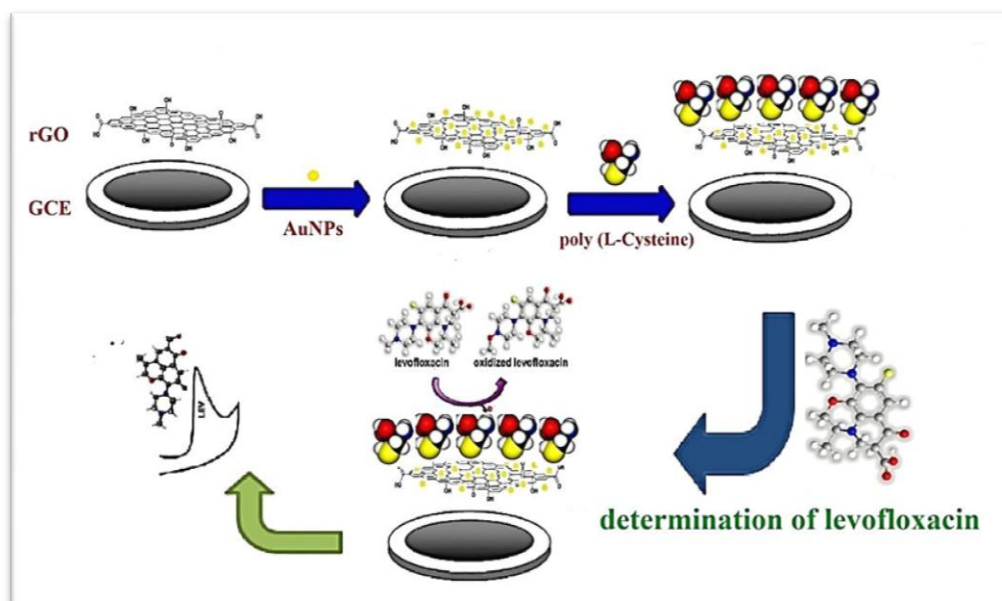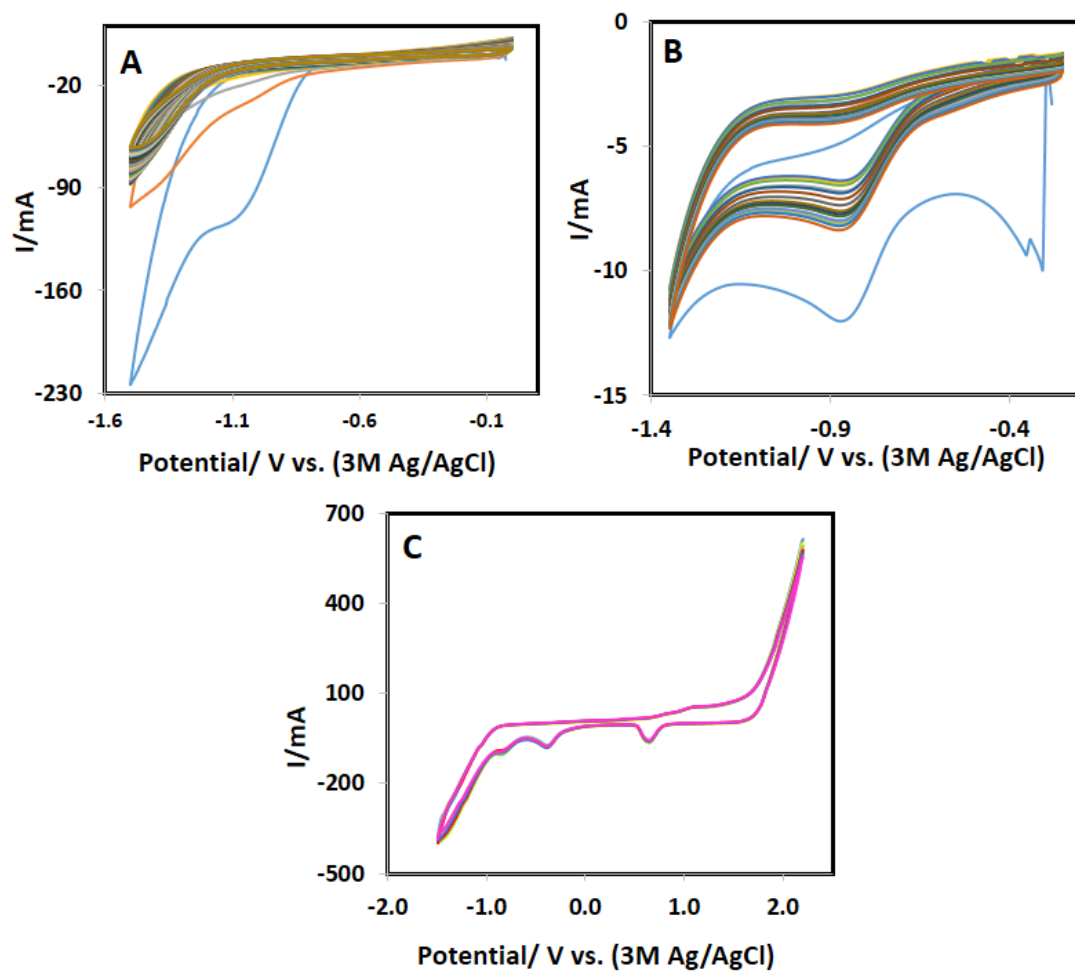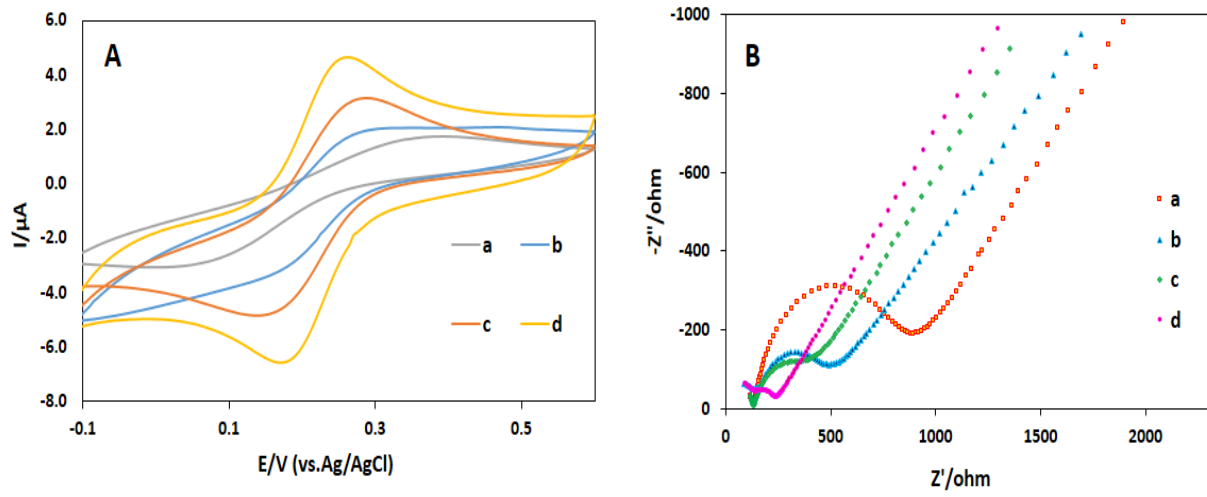
Scheme 1
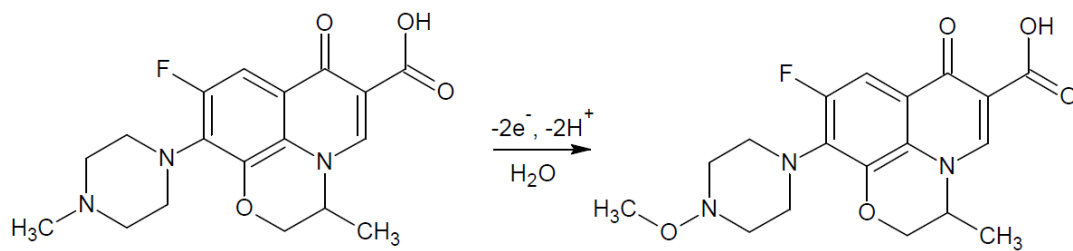
Scheme 2
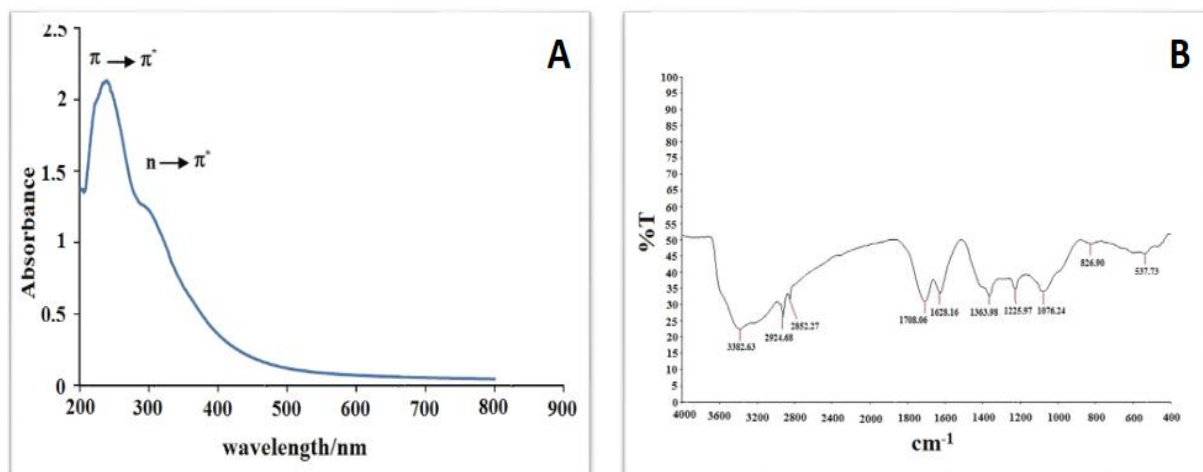
Fig. 1

Fig. 2

Fig. 3
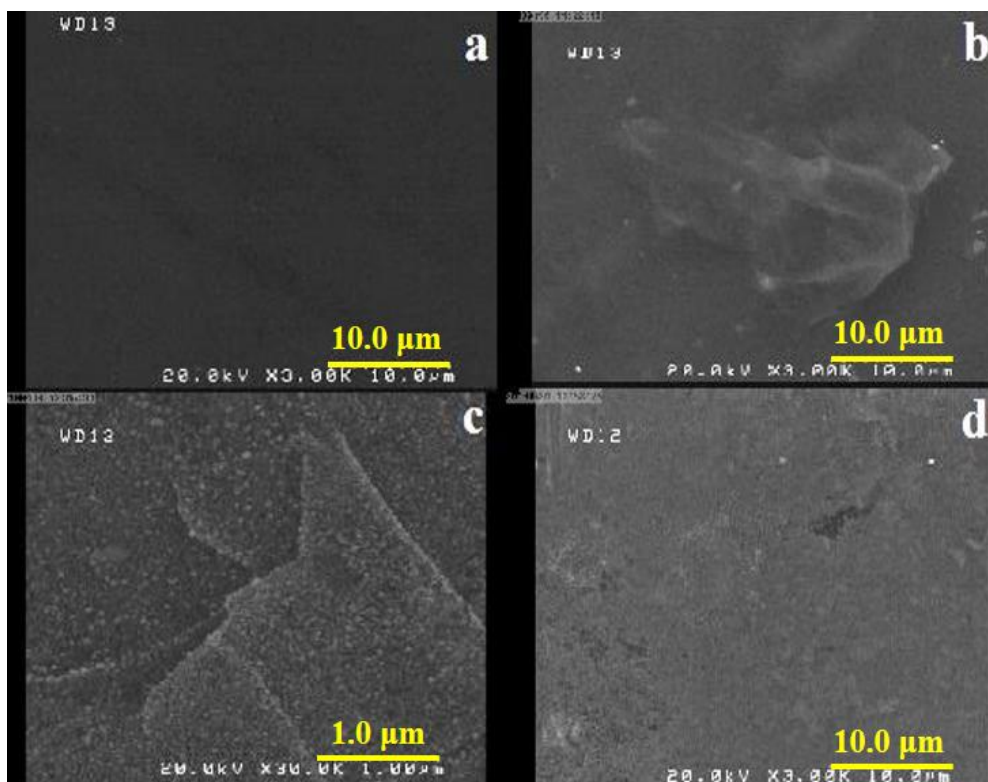
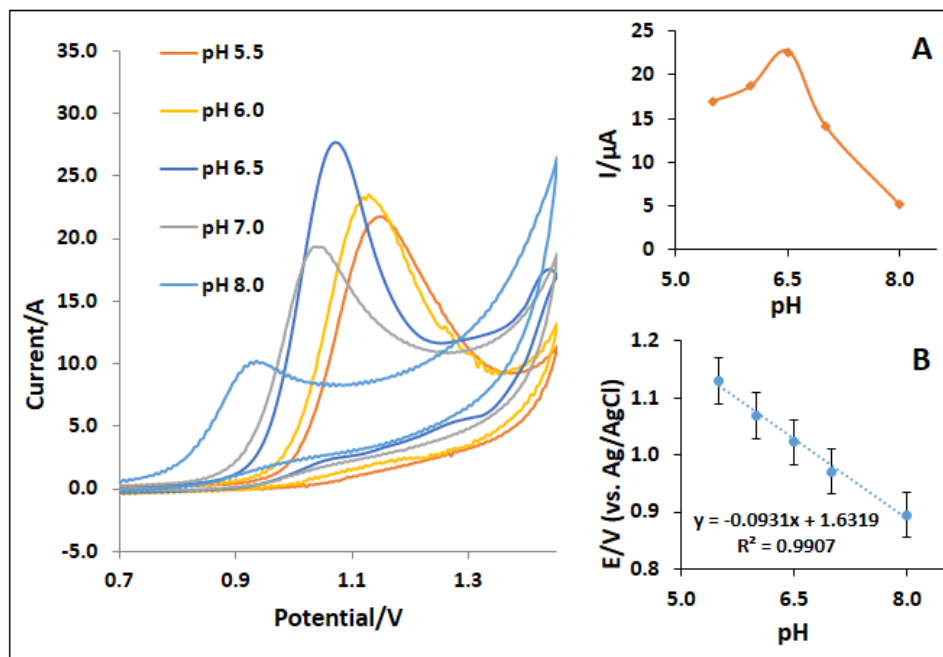**Fig. 4**
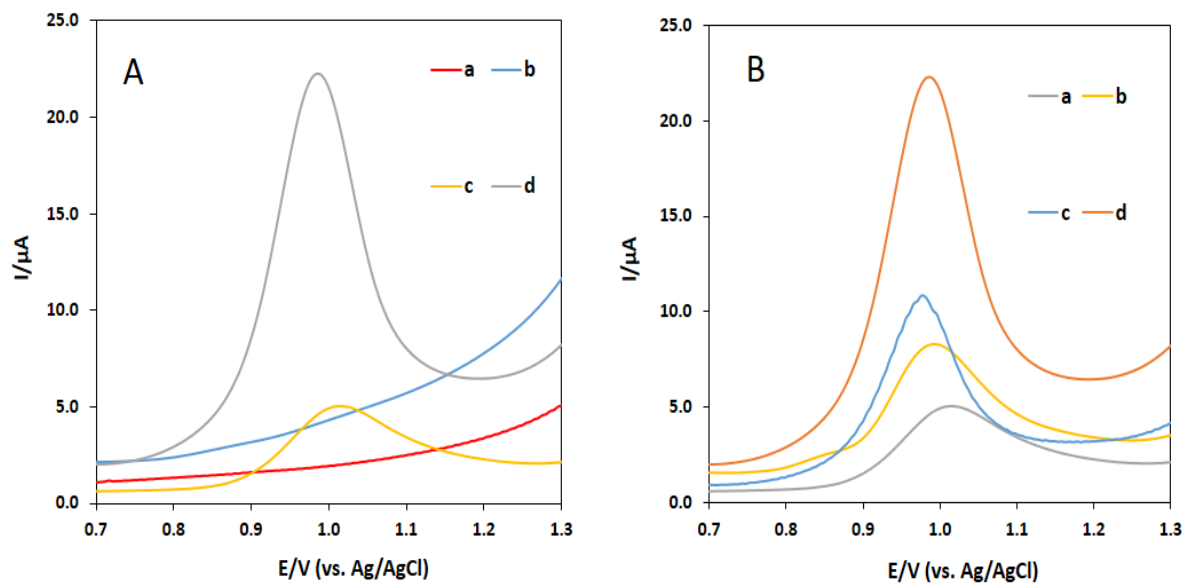
Fig. 5
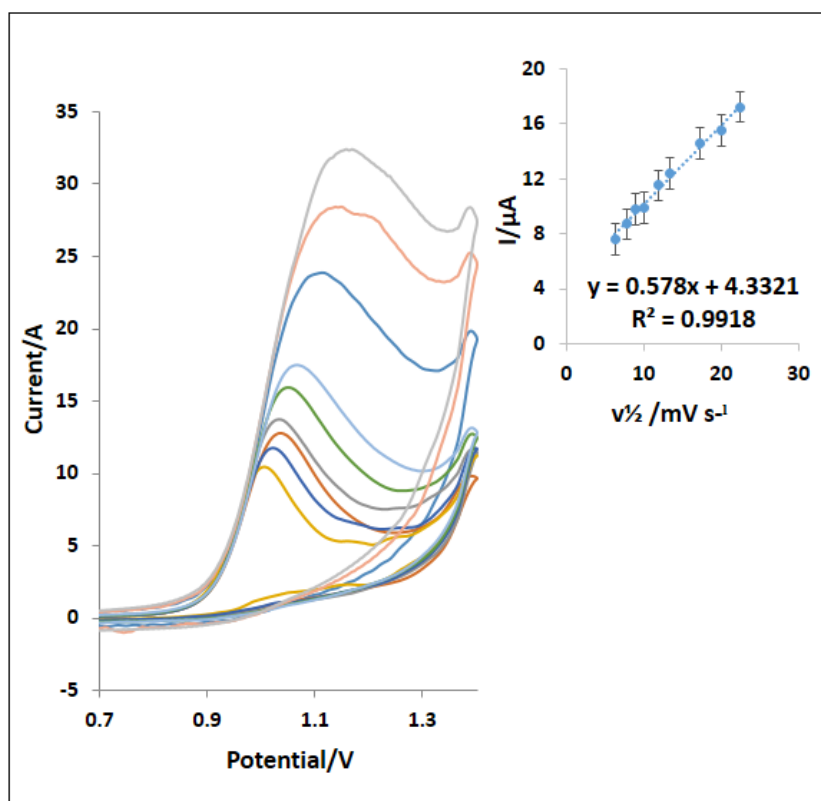
Fig. 6

Fig. 7

Fig. 8

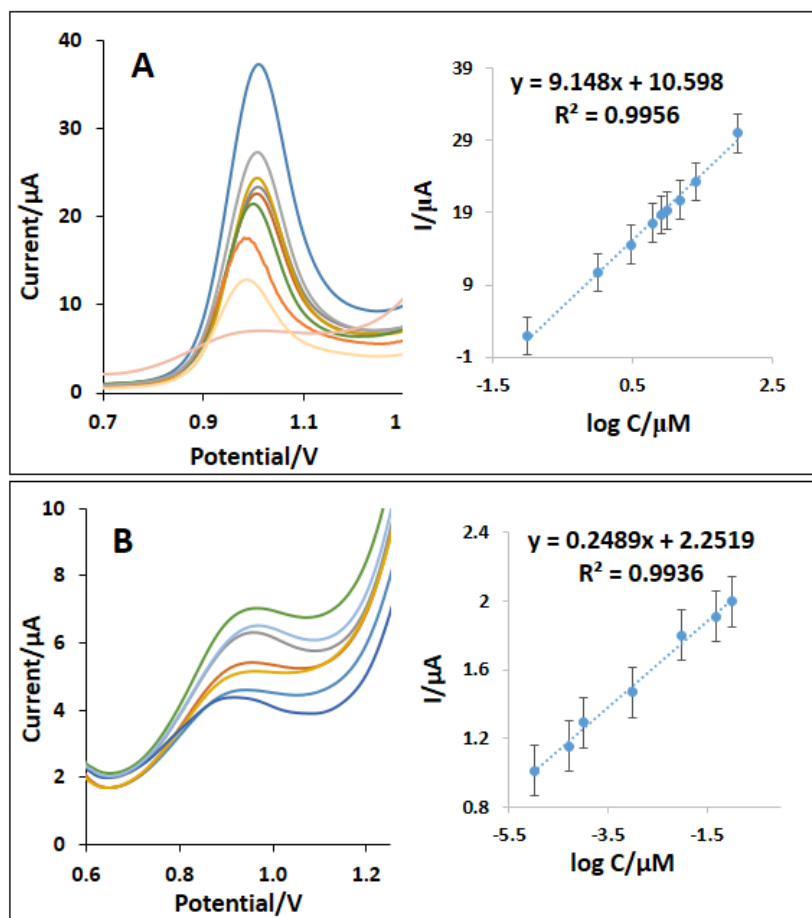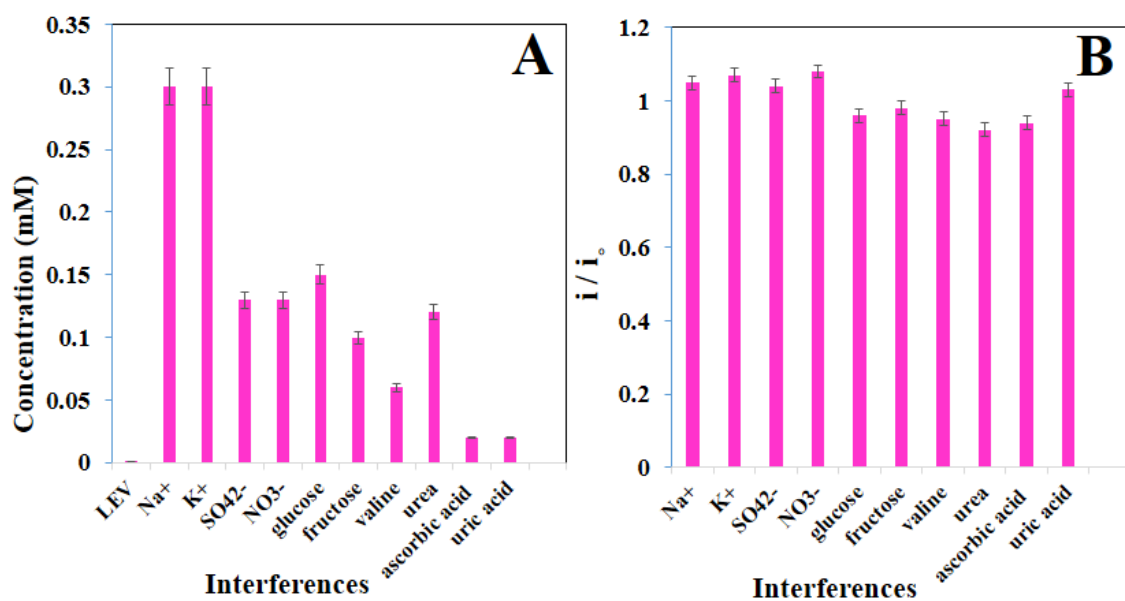**Fig. 9**

Table 1: Comparison of repeatability and stability for determination of LEV at various modified electrodes.

Electrode	repeatability			stability			Ref.
	LEV conc. (µM)	successive determinations	RSD%	LEV conc. (µM)	successive times	current response	
PoAP/MWCNTs/GCE	10.0	7	2.3	in 0.1 M H$_2$SO$_4$	30 days	91.2	[43]
AgNPs/CeO2-Au/GCE	0.1, 0.5, 5.0, 10.0	10	< 3.54	1.0	30 days	91.1	[44]
poly(p-ABSA)- rGO /GCE	-	-	-	50.0	30 days	No observable change occurred	[45]
GCE/rGO/AuNPs/ Poly(l-cys)	1.0	8	1.8	1.0	20 days	88.0	**This work**

Table 2: Comparison of analytical parameters for determination of LEV at various modified electrodes.

Electrode	Technique	Potential (V)	Liner range (µM)	LOD(µM)	Ref.
DsDNA/GCE	DPV	0.82	0.5 - 5	0.1	[46]
PDDA-rGO/gold nanoparticles	DPV	1.12, 1.26	10.0–200.0; 200.0–800.0	3.9	[47]
ssDNA/SWCNT/gold E	DPV	0.82	1.0 - 10	0.0752	[48]
MWCNTs/poly(oaminophenol) composite film	DPV	~ 1.1	3.0–200.0	1.0	[43]
MWCNT-SnO2/GC	DPV	0.91	1.0 – 9.9	0.2	[49]
MIP/G-AuNPs	DPV	1.11	1.0– 100.0	0.53	[50]
GCE/rGO/AuNPs/Poly(l-cys)	DPV CV	~ 0.91 ~ 1.1	0.00001-0.1; 0.1-100	0.000003	This work

Table 3: The application of proposed sensor for determination of LEV in human blood serum samples.

No.	LEV added (μM)	LEV found (μM)	(%) Recovery
1	4.00	3.84	96
2	8.00	7.92	99
3	12.00	12.24	102

Highlights

- The sensor shows sensitive behavior for levofloxacin

- The detection limit reached 3.0×10^{-12} M in a wide linear range from 1.0×10^{-4} M to 1.0×10^{-11} M

- The GCE modified was found to offer high stability, reproducibility, and repeatability

32